Radial flow from electromagnetic probes and signal of quark gluon plasma

Payal Mohanty, Jajati K. Nayak, Jan-e Alam, and Santosh K. Das
Variable Energy Cyclotron Centre, 1/AF, Bidhan Nagar, Kolkata 700064, India
(Received 1 June 2010; revised manuscript received 17 July 2010; published 7 September 2010)

An attempt has been made to extract the evolution of radial flow from the analysis of the experimental data on electromagnetic probes measured at the energies available at the CERN Super Proton Synchrotron (SPS) and the BNL Relativistic Heavy Ion Collider (RHIC). The transverse momentum (p_T) spectra of photons and dileptons measured by the WA98 and NA60 Collaborations, respectively, at the SPS and the photon and dilepton spectra obtained by the PHENIX Collaboration at the RHIC have been used to constrain the theoretical models. We use the ratio of photon to dilepton spectra to extract the flow, where some model dependence is canceled out. Within the ambit of the present analysis we argue that the variation of the radial velocity with invariant mass is indicative of a phase transition from the initially produced partons to hadrons at SPS and RHIC energies.

DOI: 10.1103/PhysRevC.82.034901 PACS number(s): 25.75.Dw, 12.38.Mh, 24.85.+p

I. INTRODUCTION

The hot and dense matter expected to be formed in the partonic phase after ultrarelativistic heavy-ion collisions dynamically evolves in space and time due to high internal pressure. Consequently the system cools and reverts back to hadronic matter from the partonic phase. Just after the formation, the entire energy of the system is thermal in nature and with time some part of the thermal energy gets converted to the collective (flow) energy. In other words, during the expansion stage the total energy of the system is shared by the thermal as well as the collective degrees of freedom. The evolution of the collectivity within the system is sensitive to the equation of state (EoS). Therefore, the study of the collectivity in the system formed in the quark gluon plasma (QGP) phase will be useful to shed light on the EoS [1–3] (see Refs. [4,5] for review) and on the nature of the transition that may take place during the evolution process. It is well known that the average magnitude of radial flow at the freeze-out surface can be extracted from the transverse momentum (p_T) spectra of the hadrons. However, hadrons, being strongly interacting objects, can bring the information of the state of the system when it is too dilute to support collectivity; that is, the parameters of collectivity extracted from the hadronic spectra are limited to the evolution stage where the collectivity ceases to exist. These collective parameters have hardly any information about the interior of the matter. However, electromagnetic (EM) probes, that is, photons and dileptons, are produced and emitted [6–8] (see Refs. [9–11] for review) from each space-time point. Therefore, estimating radial flow from the EM probes will shed light on the time evolution of the collectivity in the system [12].

The invariant momentum distribution of photons produced from a thermal source depends on the temperature (T) of the source through the thermal phase-space distributions of the participants of the reaction that produces the photon [13]. As a result the p_T spectra of photons reflect the temperature of the source. Hence ideally the photons with intermediate p_T values (∼2–3 GeV, depending on the value of initial temperature) reflect the properties of QGP (realized when $T > T_c$, T_c is the transition temperature). Therefore, one should look into the p_T spectra for these values of p_T for the detection of QGP. However, for an expanding system the situation is far more complex. The thermal phase-space factor changes several factors; for example, the transverse kick received by low-p_T photons due to flow originating from the low-temperature hadronic phase (realized when $T < T_c$) populates the high-p_T part of the spectra [14]. As a consequence the intermediate or the high-p_T part of the spectra contains contributions from both QGP and hadrons. For dileptons the situation is, however, different because in this case we have two kinematic variables: of these two, the p_T spectra is affected by the flow; however, the p_T integrated invariant mass (M) spectra is unaltered by the flow in the system. It should be mentioned here that, for M below the ρ peak and above the ϕ peak, dileptons from QGP dominate over its hadronic counterpart (assuming the contributions from hadronic cocktails are subtracted out) within the framework of the present model. However, the spectral function of low-mass vector mesons (mainly ρ) may shift toward lower invariant mass region due to nonzero temperature and density effects. As a consequence the contributions from the decays of such vector mesons to lepton pairs could populate the low-M window and may dominate over the contributions from the QGP phase [15] (and see also Refs. [10,11] for review). In the present work such thermal effects are not considered. All these suggest that a judicious choice of p_T and M windows will be very useful to characterize the flow in QGP and the hadronic phase. However, there are still some difficulties. The calculations of EM probes from thermal sources depend on the parameters like initial temperature (T_i), thermalization time (τ_i), chemical freeze-out temperature ($T_{\rm ch}$), kinetic freeze-out temperature (T_f), etc., which are not known uniquely. To minimize the dependence of thermal sources on these parameters, the importance of the ratio of the transverse momentum spectra of photons to dileptons has been emphasized previously [16–18] to overcome the previously mentioned uncertainties. It may be mentioned here that in the limit of $M \to 0$, the lepton pairs (virtual photons) emerge as real photons. Therefore, the evaluation of the ratio of the p_T spectra of photons to dileptons for various invariant mass bins along with a judicious choice of the p_T and M windows will

be very useful to extract the properties of QGP as well as that of the hadronic phase. This is demonstrated in the present work by analyzing photon spectra of the WA98 and PHENIX Collaborations and dilepton spectra of the NA60 and PHENIX Collaborations.

The article is organized as follows. In the next section, the production of thermal photons and dileptons is briefly outlined. In Sec. III the expansion dynamics of the system is discussed. Section IV is devoted to results and discussions and, finally, in Sec. V, we present a summary and conclusions.

II. PHOTONS AND DILEPTONS PRODUCTION

The p_T and M spectra of EM probes measured in the experiments are mingled with all the sources of production, broadly categorized as (i) prompt production resulting from the interactions of the partons of the colliding nuclei, (ii) thermal production from the interactions of thermal partons as well as from thermal hadrons, and (iii) finally production from the decays of the long-lived (compared to strong interaction time scale) mesons. The contributions from pp collisions at a given collision energy can be used as a bench-mark to estimate the hard contributions. To estimate the thermal contributions we adopt the following procedure: *thermal contributions* = *contributions from heavy-ion collision minus* $N_{\rm coll} \times$ *contributions from pp collisions*, where $N_{\rm coll}$ is the number of nucleon-nucleon interactions in the nuclear collisions at a given centrality. Instead of evaluating the hard contributions by applying perturbative QCD we use the experimental data for both photons and dileptons from the pp collisions wherever available to minimize the uncertainties in the contributions of category (i).

For collisions with large nuclei, for example, Au + Au or Pb + Pb, the number of valence d quarks are more than the number of valence u quark because in these nuclei there are more neutrons than protons. The magnitude of electric charge of the d quarks is half of that of the u quarks. Consequently, in the production of EM probes from Au + Au collisions, a larger number of d quarks with lesser charges and comparatively a smaller number of u quarks with larger charges are involved. Therefore, the photon production from Au + Au interaction for category (i) is not a mere superposition of the yield from $p + p$ interaction. However, in the present work we concentrate on the kinematic region of central rapidity where the number of valence quarks is small. In fact, this is negligible for RHIC energy. It is worth mentioning here that the role of EM probes produced from other mechanisms, like fragmentation of high-energy quarks and the interaction of high-energy partons with thermal QGP medium [19], is ignored here. It is expected that, at the p_T domain of our interest, omission of these mechanisms will not change the final results significantly.

A. Production of thermal photons and dileptons

For the present work photons and dileptons from thermalized matter of partons and hadrons play the most crucial role. The rate of thermal dilepton production per unit space-time volume per unit four-momentum volume is given by [6–9]

$$\frac{dR}{d^4p} = \frac{\alpha}{12\pi^4 p^2} L(p^2)\,\mathrm{Im}\Pi^{R\mu}_{\mu}\, f_{BE}, \tag{1}$$

where α is the EM coupling constant, $\mathrm{Im}\Pi^{\mu}_{\mu}$ is the imaginary part of the retarded photon self-energy, and $f_{BE}(E,T)$ is the thermal phase-space distribution for bosons. $L(p^2) = (1 + 2m^2/p^2)\sqrt{1-4m^2/p^2}$ arises from the final-state leptonic current involving Dirac spinors of mass m. As mentioned before, in the limit of vanishing M, a lepton pair, that is, a virtual photon, appears as a real photon. Therefore, the real photon production rate can be obtained from the dilepton emission rate by replacing the product of the EM vertex $\gamma^\star \to l^+l^-$, the term involving final-state leptonic current, and the square of the (virtual) photon propagator by the polarization sum for the real photon. For an expanding system E should be replaced by $u_\mu p^\mu$, where p^μ and u^μ are the four-momentum and the hydrodynamic four-velocity, respectively.

B. Thermal photons

The hard thermal loop [20] approximation has been used by several authors [21] to evaluate the photon spectra originating from a thermal source of quarks and gluons. The complete calculation of the emission rate of photons from QGP to order $O(\alpha\alpha_s)$ has been done by resuming ladder diagrams in the effective theory [22], which has been used in the present work. A set of hadronic reactions with all possible isospin combinations has been considered for the production of photons [23–25] from hadronic matter. The effect of hadronic dipole form factors has been taken into account in the present work like in Ref. [25].

C. Thermal dileptons

The lowest-order process producing lepton pairs is q and $\bar{q}$ annihilation. The correction of order $\alpha_s\alpha^2$ to the lowest-order rate of dilepton production from QGP has been calculated in Refs. [26,27] and is considered in the present work. For the low-M dilepton production from the hadronic phase the decays of the light vector mesons ρ, ω, and ϕ have been considered in Refs. [10,11,28]. The continuum part of the vector-meson spectral functions constrained by experimental data [28] has been included here. As mentioned before the contributions from the QGP phase dominates the M spectra of the lepton pairs below the ρ peak and above the ϕ peak if no thermal effects of the spectral functions of the vector mesons (see Refs. [10,11,29] for review) are considered. Because the continuum part of the vector-meson spectral functions are included in the current work, processes like four-pion annihilations [30] are excluded to avoid double counting.

III. EXPANSION DYNAMICS

The space-time evolution of the system formed in heavy-ion collisions has been studied by using relativistic hydrodynamics with longitudinal boost invariance [31] and cylindrical

TABLE I. The values of various parameters—thermalization time (τ_i), initial temperature (T_i), and hadronic multiplicity dN/dy—used in the present calculations.

$\sqrt{s_{NN}}$	Centrality	$\frac{dN}{dy}$	τ_i (fm)	T_i (MeV)
17.3 GeV	0%–06%	700	1.0	200
200 GeV	0%–20%	496	0.6	227
	20%–40%	226	0.6	203
	Min. bias	184	0.6	200

symmetry [32]. We assume that the system reaches equilibration at a time τ_i after the collision. The initial temperature, T_i can be related to the measured hadronic multiplicity (dN/dy) by the following relation:

$$T_i^3 \tau_i \approx \frac{2\pi^4}{45\zeta(3)} \frac{1}{4a_{\text{eff}}} \frac{1}{\pi R_A^2} \frac{dN}{dy}, \tag{2}$$

where R_A is the radius of the system, $\zeta(3)$ is the Riemann zeta function, and $a_{\text{eff}} = \pi^2 g_{\text{eff}}/90$, where g_{eff} $(= 2 \times 8 + 7 \times 2 \times 2 \times 3 \times N_F/8)$ is the degeneracy of quarks and gluons in QGP (N_F = number of flavors). The values of dN/dy for various beam energies and centralities are calculated from the following equation [33],

$$\frac{dN}{dy} = (1-x)\frac{dn_{pp}}{dy}\frac{\langle N_{\text{part}}\rangle}{2} + x\frac{dn_{pp}}{dy}\langle N_{\text{coll}}\rangle, \tag{3}$$

and tabulated in Table I.

N_{coll} is the number of collisions and contributes the x fraction to the multiplicity dn_{pp}/dy measured in the pp collision. The number of participants, N_{part}, contributes fraction $(1-x)$ of dn_{pp}/dy. The values of N_{part} and N_{coll} are estimated by using the Glauber model and the results are in agreement with Ref. [34]. We have used $dn_{pp}/dy = 2.43$ and $x = 0.1$ at $\sqrt{s_{NN}} = 200$ GeV. It should be mentioned here that the values of dN/dy [through N_{part} and N_{coll} in Eq. (3)] and hence the T_i [through dN/dy in Eq. (2)] depend on the centrality of the collisions. The values of R_A for different centralities have been evaluated by using the equation $R_A \sim 1.1 N_{\text{part}}^{1/3}$. Some comments are in order here regarding the flow for noncentral collisions that results in the noncylindrical geometrical shape of the system formed after the collisions. In the present work the noncentrality of the nuclear collisions is reflected in the initial temperature through hadronic multiplicity. The geometry of the system due to noncentrality should, in principle, be treated by $(2+1)$ dimensional [35] evolution or for more rigorous treatment $(3+1)$ dimensional hydrodynamical [36] evolution. However, we expect that the results obtained in the present work will not be affected substantially due to the noncylindrical geometric shape of the system, because the flow has been extracted from the ratio of photon to dilepton spectra for a given centrality.

We use the EoS obtained from the lattice QCD calculations by the MILC Collaboration [37]. We consider the kinetic freeze-out temperature, $T_f = 140$ MeV, for all the hadrons. The ratios of various hadrons measured experimentally at different $\sqrt{s_{NN}}$ indicate that the system formed in heavy-ion collisions chemically decouple at T_{ch}, which is higher than T_f, which can be determined by the transverse spectra of hadrons [38]. Therefore, the system remains out of chemical equilibrium from T_{ch} to T_f. The deviation of the system from the chemical equilibrium is taken into account by introducing the chemical potential for each hadronic species. The chemical nonequilibration affects the yields through the phase-space factors of the hadrons, which in turn affects the production of the EM probes. The value of the chemical potential has been taken into account following Ref. [3]. It is expected that the chemical potentials do not change much with the inclusion of resonances above Δ.

IV. RESULTS AND DISCUSSION

A. p_T distributions of photons and dileptons

The prompt photons and dileptons (Drell-Yan) are normally estimated by using perturbative QCD. However, to minimize the theoretical model dependence here we use the available experimental data from pp collisions to estimate the hard photon and dilepton contributions in heavy-ion collisions. The WA98 photon spectra from Pb + Pb collisions is measured at $\sqrt{s_{NN}} = 17.3$ GeV. However, no data at this collision energy are available for pp interactions. Therefore, prompt photons for $p+p$ collisions at $\sqrt{s_{NN}} = 19.4$ GeV have been used [39] to estimate the hard contributions for nuclear collisions at $\sqrt{s_{NN}} = 17.3$ GeV. The appropriate scaling (see Ref. [40] for details) has been used to obtain the results at $\sqrt{s_{NN}} = 17.3$ GeV. For the Pb + Pb collisions the result has been appropriately scaled by the number of collisions at this energy (this is shown in Fig. 1 as prompt photons). The high-p_T part of the WA98 data is reproduced by the prompt contributions reasonably well. At low-p_T the hard contributions underestimate the data indicating the presence of a thermal source. The thermal photons with an initial temperature of 200 MeV along with the prompt contributions explain the WA98 data well (Fig. 1), with the inclusion of nonzero chemical potentials for all hadronic species considered [3] (see also Ref. [41]). In some of the previous works [42–47], the effect of chemical freeze-out is ignored. As a result either a higher value of T_i or a substantial reduction of hadronic masses in the

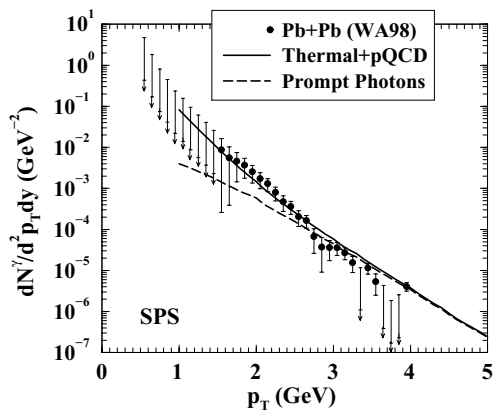

FIG. 1. Transverse momentum spectra of photons at SPS energy for Pb + Pb collisions at midrapidity.

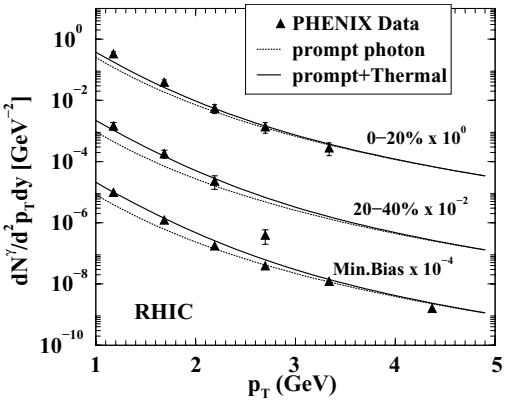

FIG. 2. Transverse momentum spectra of photons at RHIC energy for Au-Au collisions for different centralities at midrapidity.

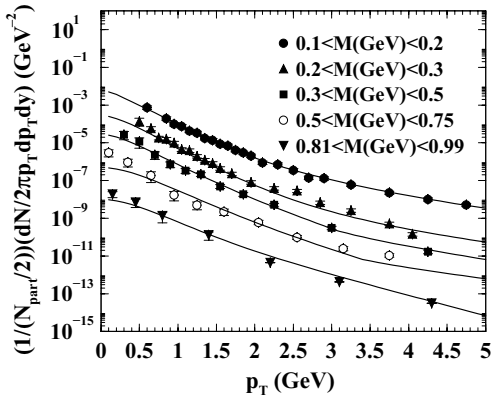

FIG. 4. Transverse momentum spectra of dileptons for different invariant mass windows for minimum bias Au-Au collisions at RHIC energies.

medium was required [42]. In the present work, the data have been reproduced without any such effects.

Following a similar procedure, the data [48] from Au-Au collisions at $\sqrt{s_{NN}} = 200$ GeV have been reproduced well by adding the prompt contributions (which is constrained by pp data at the same energy) to the thermal photons. The reproduction of data is satisfactory (Fig. 2) for all the centralities with the initial temperature shown in Table I (see also Ref. [49]).

The transverse mass distribution of dimuons produced in In + In collisions at $\sqrt{s_{NN}} = 17.3$ GeV has been evaluated for different invariant mass ranges (see Ref. [50] for details). The quantity $dN/M_T dM_T$ has been obtained by integrating the production rates over invariant mass windows $M_{\min}$ to $M_{\max}$ and M_T is defined as $\sqrt{\langle M\rangle 2 + p_T^2}$, where $\langle M\rangle = (M_{\min} + M_{\max})/2$. The results are compared with the data obtained by the NA60 Collaboration [51] at SPS energies (Fig. 3). Theoretical results contain contributions from the thermal decays of light vector mesons (ρ, ω, and ϕ) and also from the decays of vector mesons at the freeze-out [52] of the system. The nonmonotonic variation of the effective slope parameter extracted from the M_T spectra of the lepton pair with $\langle M\rangle$ evaluated within the ambit of the present model [50] reproduces the NA60 [51] results reasonably well. For Au + Au collisions at $\sqrt{s_{NN}} = 200$ GeV, we have evaluated the dilepton spectra for different invariant mass bins with the initial condition (min. bias) shown in Table I and the lattice QCD equation of state. The results are displayed in Fig. 4. The slopes of the experimental data on p_T distribution of lepton pairs for different invariant mass windows measured by the PHENIX Collaboration [53] could be reproduced well with the same initial condition that reproduces photon spectra [48]. In fact, the reproduction of data for the higher mass windows $0.5 < M\,(\text{GeV}) < 0.75$ and $0.81 < M\,(\text{GeV}) < 0.99$ do not need any normalization factors (Fig. 4). For lower mass windows, slopes are reproduced well but fail to reproduce the absolute normalization. Therefore, it should be clarified here that the theoretical results shown in Fig. 4 for lower mass windows (to be precise for $0.1 < M\,(\text{GeV}) < 0.2$, $0.2 < M\,(\text{GeV}) < 0.3$, and $0.3 < M\,(\text{GeV}) < 0.5$) contain arbitrary normalization constants. However, it should also be mentioned at this point that for the extraction of the flow within the present approach the absolute normalization is not essential, what is essential is the slope [Eq. (5)]. Therefore, the nonreproduction of the absolute normalization of the p_T spectra of lepton pairs for the lower mass windows does not affect the extraction of the magnitude of the radial flow.

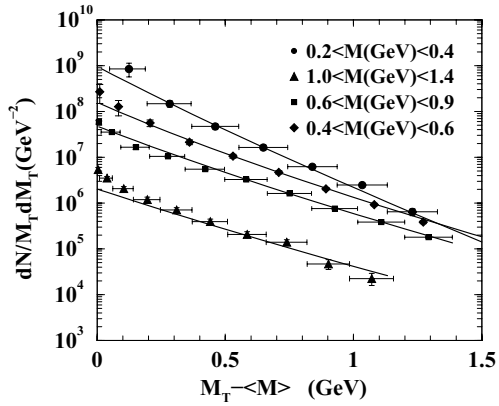

FIG. 3. Transverse mass spectra of dimuons in In + In collisions at SPS energies. Solid lines denote the theoretical results.

B. The ratio, R_{em}

As mentioned before some of the uncertainties prevailing in the individual spectra may be removed by taking the ratio, R_{em}, of the p_T distribution of thermal photons to dileptons. In the absence of experimental data for both photons and dileptons from the same colliding system for SPS energies, we have calculated the ratio R_{em} for the Pb + Pb system, where the initial condition, the freeze-out condition, and the EoS are constrained by the measured WA98 photon spectra. The results are displayed in Fig. 5.

Next we evaluate the ratio of the thermal photon to dilepton spectra constrained by the experimental data from Au + Au collisions measured by the PHENIX Collaboration. The results for the thermal ratio R_{em} displayed in Fig. 6 are constrained by the experimental data. The behavior of R_{em} with p_T for different invariant mass windows, which is

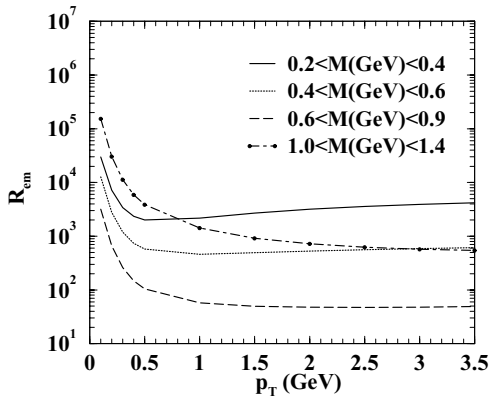

FIG. 5. Variation of thermal photon to dilepton ratio, $R_{\rm em}$, with p_T for different invariant mass windows at SPS energies (see text).

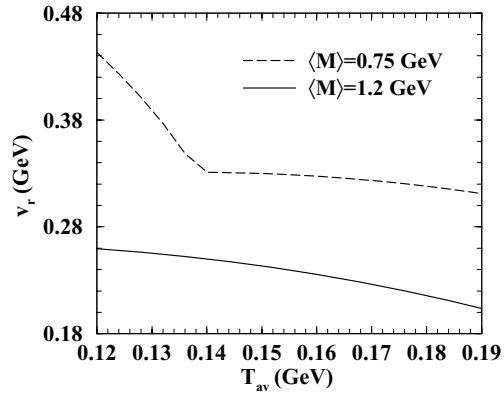

FIG. 7. The variation of radial flow velocity with average temperature of the system for $\langle M\rangle = 0.75$ GeV and 1.2 GeV at SPS energies.

extracted from the available data, is similar to the theoretical results obtained in Ref. [17].

The ratio $R_{\rm em}$ for different M windows (Figs. 5 and 6) can be parametrized as follows:

$$R_{\rm em} = A\left(\frac{M_T}{p_T}\right)^B \exp\left(\frac{M_T - p_T}{T_{\rm eff}}\right), \tag{4}$$

with different values of $T_{\rm eff}$ for different invariant mass windows. The argument of the exponential in Eq. (4) can be written as [18]

$$\frac{M_T - p_T}{T_{\rm eff}} = \frac{M_T}{T_{\rm eff2}} - \frac{p_T}{T_{\rm eff1}} = \frac{M_T}{T_{\rm av} + M v_r^2} - \frac{p_T}{T_{\rm av}\sqrt{\frac{1+v_r}{1-v_r}}}, \tag{5}$$

where $T_{\rm eff1} = T_{\rm av}\sqrt{\frac{1+v_r}{1-v_r}}$ is the blue shifted effective temperature for massless photons and $T_{\rm eff2} = T_{\rm av} + M v_r^2$ is the effective temperature for massive dileptons. $T_{\rm av}$ is the average temperature and v_r is the average radial flow of the system. For a given p_T and M, Eq. (5) can be written as $v_r = f(T_{\rm av})$. The $T_{\rm eff}$ obtained from the parametrization of the ratio at SPS energies are 263 MeV and 243 MeV for $M = 0.75$ and 1.2 GeV, respectively. The average flow velocity v_r versus $T_{\rm av}$ is displayed for $M = 0.75$ GeV and 1.2 GeV in Fig. 7. The hadronic matter (QGP) dominates the $M \sim 0.75(1.2)$ GeV region. Therefore, these two mass windows are selected to extract the flow parameters for the respective phases. The v_r increases with decreasing $T_{\rm av}$ (increase in time) and reaches its maximum when the temperature of the system is minimum, that is, when the system attains T_f, the freeze-out temperature. Therefore, the variation of v_r with $T_{\rm av}$ may be treated so as to show how the flow develops in the system. The v_r is larger in the hadronic phase because the velocity of sound in this phase is smaller, which makes the expansion slower, and as a consequence the system lives longer—allowing the flow to fully develop. However, v_r is smaller in the QGP phase because it has a smaller lifetime where the flow is only partially developed. In Fig. 8 the variation of average transverse velocity with average temperature for RHIC initial conditions is depicted. The magnitude of the flow is larger in the case of RHIC than SPS because of the higher initial pressure. Because of the larger initial pressure and QGP lifetime, the radial velocity for QGP at RHIC is larger compared to that at SPS.

Obtaining $T_{\rm eff1}$ and $T_{\rm eff2}$ from the individual spectra and eliminating $T_{\rm av}$ one gets the variation of v_r with M. Figure 9 (left panel) shows the variation of v_r with M for SPS

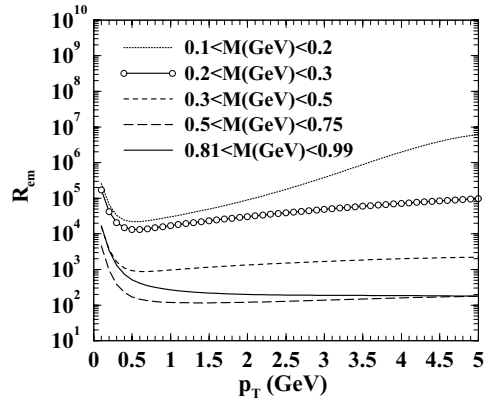

FIG. 6. Variation of thermal photon to dilepton ratio, $R_{\rm em}$, with p_T for different invariant mass windows at RHIC energies (see text).

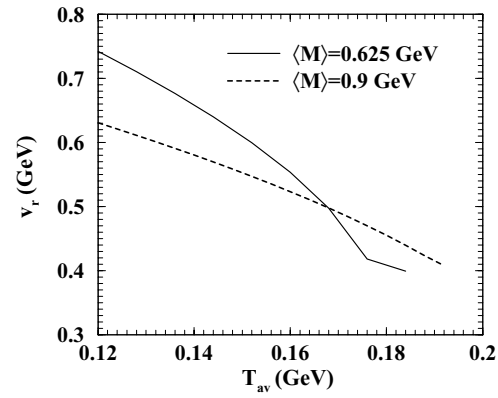

FIG. 8. The variation of radial flow velocity with average temperature of the system for $\langle M\rangle = 0.625$ GeV and 0.9 GeV at RHIC energies.

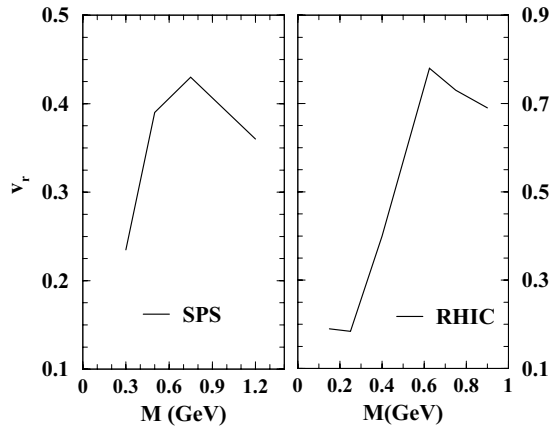

FIG. 9. The variation of radial flow with invariant mass pairs for SPS (left) and RHIC (right) energies.

conditions. The radial flow velocity increases with invariant mass M up to $M = M_\rho$ and then drops. How can we understand this behavior? From the invariant mass spectra it is well known that the low-M (below ρ mass) and high-M (above ϕ peak) pairs originate from a partonic source [17]. The collectivity (or flow) does not develop fully in the QGP because of the small lifetime of this phase, which means that the radial velocity in QGP will be smaller for both low and high M. The lepton pairs with mass around the ρ peak mainly originate from a hadronic source (at a late stage of the evolution of system) and are largely affected by the flow, resulting in higher values of flow velocity. In summary, the value of v_r for M below and above the ρ peak is small but around the ρ peak is large—with the resulting behavior displayed in Fig. 9. Similar nonmonotonic behavior is observed in the case of elliptic flow of photons as a function of p_T [54]. The variation of v_r with M at RHIC (Fig. 9, right panel) is similar to that at SPS, though the values of v_r at RHIC are larger than those at SPS as expected due to higher initial pressure.

V. SUMMARY AND CONCLUSIONS

The photon and dilepton spectra measured at SPS and RHIC energies by different experimental collaborations have been studied. The initial conditions have been constrained to reproduce the measured multiplicity in these collisions. The EoS, the other crucial input to the calculations, has been taken from lattice QCD calculations. The deviation of the hadronic phase from chemical equilibrium is taken into account by introducing nonzero chemical potentials for each hadronic species. It is shown that simultaneous measurements of photon and dilepton spectra in heavy-ion collisions will enable us to quantify the evolution of the average radial flow velocity for the system, and the nature of the variation of radial flow with invariant mass indicates the formation of partonic phases at SPS and RHIC energies.

ACKNOWLEDGMENTS

We are grateful to Tetsufumi Hirano for providing us the hadronic chemical potentials. This work is supported by the DAE-BRNS Project, Sanction No. 2005/21/5-BRNS/2455.

[1] E. Schnedermann, J. Sollfrank, and U. Heinz, Phys. Rev. C **48**, 2462 (1993).
[2] C. M. Hung and E. Shuryak, Phys. Rev. C **57**, 1891 (1998).
[3] T. Hirano and K. Tsuda, Phys. Rev. C **66**, 054905 (2002).
[4] P. Huovinen and P. V. Ruuskanen, Annu. Rev. Nucl. Part. Sci. **56**, 163 (2006).
[5] D. A. Teaney, arXiv:0905.2433 [nucl-th].
[6] L. D. McLerran and T. Toimela, Phys. Rev. D **31**, 545 (1985).
[7] C. Gale and J. I. Kapusta, Nucl. Phys. B **357**, 65 (1991).
[8] H. A. Weldon, Phys. Rev. D **42**, 2384 (1990).
[9] J. Alam, S. Raha, and B. Sinha, Phys. Rep. **273**, 243 (1996).
[10] J. Alam, S. Sarkar, P. Roy, T. Hatsuda, and B. Sinha, Ann. Phys. **286**, 159 (2000).
[11] R. Rapp and J. Wambach, Adv. Nucl. Phys. **25**, 1 (2000).
[12] T. Renk and J. Ruppert, Phys. Rev. C **77**, 024907 (2008).
[13] C. Y. Wong, *Introduction to High Energy Heavy Ion Collisions* (World Scientific, Singapore, 1994).
[14] J. Alam, D. K. Srivastava, B. Sinha, and D. N. Basu, Phys. Rev. D **48**, 1117 (1993).
[15] J. Ruppert, C. Gale, T. Renk, P. Lichard, and J. I. Kapusta, Phys. Rev. Lett. **100**, 162301 (2008).
[16] B. Sinha, Phys. Lett. B **128**, 91 (1983).
[17] J. K. Nayak, J. Alam, S. Sarkar, and B. Sinha, Phys. Rev. C **78**, 034903 (2008).
[18] J. K. Nayak and J. Alam, Phys. Rev. C **80**, 064906 (2009).
[19] S. Turbide, C. Gale, E. Frodermann, and U. Heinz, Phys. Rev. C **77**, 024909 (2008).
[20] E. Braaten and R. D. Pisarski, Nucl. Phys. B **337**, 569 (1990); **339**, 310 (1990).
[21] J. Kapusta, P. Lichard, and D. Seibert, Phys. Rev. D **44**, 2774 (1991); R. Bair, H. Nakkagawa, A. Niegawa, and K. Redlich, Z. Phys. C **53**, 433 (1992); P. Aurenche, F. Gelis, H. Zaraket, and R. Kobes Phys. Rev. D **58**, 085003 (1998).
[22] P. Arnold, G. D. Moore, and L. G. Yaffe, J. High Energy Phys. 11 (2001) 057; 12 (2001) 009; 06 (2002) 030.
[23] S. Sarkar, J. Alam, P. Roy, A. K. Dutt-Mazumder, B. Dutta-Roy, and B. Sinha, Nucl. Phys. A **634**, 206 (1998).
[24] P. Roy, S. Sarkar, J. Alam, and B. Sinha, Nucl. Phys. A **653**, 277 (1999).
[25] S. Turbide, R. Rapp, and C. Gale, Phys. Rev. C **69**, 014903 (2004).
[26] T. Altherr and P. V. Ruuskanen, Nucl. Phys. B **380**, 377 (1992).
[27] M. H. Thoma and C. T. Traxler, Phys. Rev. D **56**, 198 (1997).
[28] E. V. Shuryak, Rev. Mod. Phys. **65**, 1 (1993).
[29] G. E. Brown and M. Rho, Phys. Rep. **269**, 333 (1996).
[30] P. Lichard and J. Juráň, Phys. Rev. D **76**, 094030 (2007).
[31] J. D. Bjorken, Phys. Rev. D **27**, 140 (1983).
[32] H. von Gersdorff, L. D. McLerran, M. Kataja, and P. V. Ruuskanen, Phys. Rev. D **34**, 794 (1986).
[33] D. Kharzeev and M. Nardi, Phys. Lett. B **507**, 121 (2001).
[34] S. S. Adler *et al.* (PHENIX Collaboration), Phys. Rev. Lett. **91**, 072301 (2003).
[35] P. F. Kolb, J. Sollfrank, and U. Heinz, Phys. Rev. C **62**, 054909 (2000).
[36] T. Hirano, Phys. Rev. C **65**, 011901 (2001).

[37] C. Bernard *et al.*, Phys. Rev. D **75**, 094505 (2007).
[38] I. Arsene *et al.* (BRAHMS Collaboration), Nucl. Phys. A **757**, 1 (2005); B. B. Back *et al.* (PHOBOS Collaboration), *ibid.* **757**, 28 (2005); J. Adams *et al.* (STAR Collaboration), *ibid.* **757**, 102 (2005); K. Adcox *et al.* (PHENIX Collaboration), *ibid.* **757**, 184 (2005).
[39] D. L. Adams *et al.* (E704 Collaboration), Phys. Lett. B **345**, 569 (1995).
[40] M. M. Aggarwal *et al.* (WA98 Collaboration), Phys. Rev. Lett. **85**, 3595 (2000).
[41] T. Renk, Phys. Rev. C **71**, 064905 (2005); J. Phys. G **30**, 1495 (2004).
[42] J. Alam, S. Sarkar, T. Hatsuda, T. K. Nayak, and B. Sinha, Phys. Rev. C **63**, 021901(R) (2001); J. Alam, P. Roy, S. Sarkar, and B. Sinha, *ibid.* **67**, 054901 (2003).
[43] D. K. Srivastava and B. Sinha, Phys. Rev. C **64**, 034902 (2001).
[44] P. Huovinen, P. V. Ruuskanen, and S. S. Rasanen, Phys. Lett. B **535**, 109 (2002).
[45] K. Gallmeister, B. Kämpfer, and O. P. Pavlenko, Phys. Rev. C **62**, 057901 (2000).
[46] F. D. Steffen and M. H. Thoma, Phys. Lett. B **510**, 98 (2001).
[47] R. Chatterjee, D. K. Srivastava, and S. Jeon, Phys. Rev. C **79**, 034906 (2009).
[48] A. Adare *et al.* (PHENIX Collaboration), Phys. Rev. Lett. **104**, 132301 (2010).
[49] F.-M. Liu, T. Hirano, K. Werner, and Y. Zhu, Phys. Rev. C **79**, 014905 (2009).
[50] J. Alam, T. Hirano, J. K. Nayak, and B. Sinha, arXiv:0902.0446 [nucl-th].
[51] R. Arnaldi *et al.* (for NA60 Collaborations), Phys. Rev. Lett. **100**, 022302 (2008).
[52] E. Cooper and G. Frye, Phys. Rev. D **10**, 186 (1974).
[53] A. Toia (PHENIX Collaboration), J. Phys. G **35**, 104037 (2008); A. Adare *et al.* (PHENIX Collaboration), Phys. Rev. C **81**, 034911 (2010).
[54] F.-M. Liu, T. Hirano, K. Werner, and Y. Zhu, Nucl. Phys. A **830**, 587c (2009); R. Chatterjee, E. S. Frodermann, U. W. Heinz, and D. K. Srivastava, Phys. Rev. Lett. **96**, 202302 (2006).